Available online at www.sciencedirect.com

ScienceDirect

Journal of Nutritional Biochemistry 95 (2021) 108762

Journal of Nutritional Biochemistry

RESEARCH PAPER

Effects of a high-fat diet and global aryl hydrocarbon receptor deficiency on energy balance and liver retinoid status in male Sprague-Dawley rats

Raimo Pohjanvirta[a,*], Ira Karppinen[a], Suylen Galbán-Velázquez[b], Javier Esteban[b], Helen Håkansson[c], Satu Sankari[d], Jere Lindén[e]

[a] Department of Food Hygiene & Environmental Health, Faculty of Veterinary Medicine, University of Helsinki, Helsinki, Finland
[b] Instituto de Bioingeniería, Universidad Miguel Hernández de Elche, Elche, Alicante, Spain
[c] Institute of Environmental Medicine, Karolinska Institutet, Stockholm, Sweden
[d] Department of Equine and Small Animal Medicine, Faculty of Veterinary Medicine, University of Helsinki, Helsinki, Finland
[e] FCLAP, Department of Veterinary Biosciences, Faculty of Veterinary Medicine, University of Helsinki, Finland

Received 9 July 2020; received in revised form 9 February 2021; accepted 8 April 2021

Abstract

The physiological functions of the aryl hydrocarbon receptor (AHR) are only beginning to unfold. Studies in wildtype and AHR knockout (AHRKO) mice have recently disclosed that AHR activity is required for obesity and steatohepatitis to develop when mice are fed with a high-fat diet (HFD). In addition, a line of AHRKO mouse has been reported to accumulate retinoids in the liver. Whether these are universal manifestations across species related to AHR activity level is not known yet. Therefore, we here subjected wildtype and AHRKO male rats (on Sprague-Dawley background) to HFD feeding coupled with free access to 10% sucrose solution and water; controls received a standard diet and water. Although the HFD-fed rats consumed more energy throughout the 24-week feeding regimen, they did not get overweight. However, relative weights of the brown and epididymal adipose tissues were elevated in HFD-fed rats, while that of the liver was lower in AHRKO than wildtype rats. Moreover, the four groups exhibited diet- or genotype-dependent differences in biochemical variables, some of which suggested marked dissimilarities from AHRKO mice. Expression of pro- and anti-inflammatory genes was induced in livers of HFD-fed AHRKO rats, but histologically they did not differ from others. HFD reduced the hepatic concentrations of retinyl palmitate, 9-cis-4-oxo-13,14-dihydroretinoic acid and (suggestively) retinol, whereas AHR status had no effect. Hence, the background strain/line of AHRKO rat is resistant to diet-induced obesity, and AHR does not modulate this or liver retinoid concentrations. Yet, subtle AHR-dependent differences in energy balance-related factors exist despite similar weight development.

Keywords: Aryl hydrocarbon receptor; Genetically modified organisms; High-fat diet, Diet-induced obesity; Energy balance; Retinoids.

1. Introduction

The ligand-activated transcription factor aryl hydrocarbon receptor (AHR) was originally discovered as the mediator of xenobiotic-metabolizing enzyme induction by, and toxicity of, both polycyclic aromatic hydrocarbons and dioxin-like polyhalogenated compounds [1]. More recent studies have primarily focussed on its numerous physiological roles. It has been found to be involved in cell proliferation, migration and apoptosis [2,3], liver and blood vessel development [4,5], and the control of reproductive systems [6], immune responses [7] and behaviour [8]. Recently, much research has been devoted to AHR's critical participation in the maintenance of intestinal microbiome stability and mucosal integrity [9–13].

A novel action of the AHR, possibly related to its intestinal impacts, came to light a few years ago. It was unexpectedly

Abbreviations: AHR, aryl hydrocarbon receptor; AHRKO, AHR knockout; ATRA, all-*trans* retinoic acid; BAT, brown adipose tissue; CORA, 9-*cis*-4-oxo-13,14-dihydroretinoic acid; HFD, high-fat diet; ILC3, type 3 innate lymphoid cells; JAK/STAT3, Janus kinases-signal transducer and activator of transcription 3; LOD, limit of detection; LRAT, lecithin:retinol acetyltransferase; RA13C, 13-*cis*-retinoic acid; REOH, retinol; REPA, retinyl palmitate; SD, standard diet; SOCS3, suppressor of cytokine signalling 3; TCDD, 2,3,7,8-tetrachlorodibenzo-*p*- dioxin; WAT, white adipose tissue; WT, wildtype.

* Corresponding author at: Raimo Pohjanvirta, Department of Food Hygiene & Environmental Health, Faculty of Veterinary Medicine, University of Helsinki, P.O. Box 66, 00014 Helsinki, Finland, Tel.: +358-2-94157147
E-mail address: raimo.pohjanvirta@helsinki.fi (R. Pohjanvirta).

https://doi.org/10.1016/j.jnutbio.2021.108762

observed that in congenic C57BL/6J mice, differing only at the *Ahr* locus, obesity on a high-fat diet (HFD) correlated positively with the affinity of AHR to the most potent dioxin congener, 2,3,7,8-tetrachlorodibenzo-*p*-dioxin (TCDD) [14]. Subsequent studies showed that if AHR signalling was blocked or even partially inhibited by genetic or pharmacological means, HFD-induced obesity, fatty liver, glucose intolerance and insulin resistance could be prevented, while no influence of AHR status on body weight was discernible on a standard diet (SD) [15–18]. The effect seemed to principally emanate from enhanced energy expenditure, but the exact mechanism remained elusive. Additional research on tissue-specific AHRKO male mice revealed that AHR ablation in neither the liver nor the white adipose tissue (WAT) alone could reproduce the anti-obesity outcome [19,20], thus excluding these two tissues as critical sites for the effect.

The opposite physiological state to that of AHR deficiency, perpetual hyperactivation of AHR, can be brought about with TCDD. Chronic exposure to a low, sub-lethal dose of TCDD was found to augment obesity in mice on HFD [21]. Hence, gentle global AHR activation seems to favour energy conservation whereas AHR deficiency or impaired signalling promote energy expenditure and thereby protect against diet-induced obesity in mice. In contrast, extreme activation of AHR by a high (lethal) dose of TCDD to laboratory animals typically results in a wasting syndrome which entails a dramatic, up to >50% body weight loss during 2–6 weeks post-exposure, finally culminating in death [22].

In addition to energy balance, the AHR may be involved in the regulation of hepatic retinoid status, but its role there is still unclear. A study in AHRKO mice reported substantially elevated liver retinoid (all-*trans* retinoic acid [ATRA], retinol [REOH], and retinyl palmitate [REPA]) concentrations compared with their wild-type (WT) counterparts [23]. However, this finding could not be confirmed in another AHRKO mouse line [24]. Retinoids may also participate in, or contribute to, the outcomes of modified AHR function since AHR overactivation brought about by TCDD exposure leads to signs and pathologies reminiscent of vitamin A deficiency and/or vitamin A excess (discussed in further detail elsewhere [24]). Similar to the AHR, retinoic acid has proven to be essential for ILC3 development and function [25]. Because all the experimental data available at present on the impact of AHR deficiency on both energy homeostasis and liver retinoids originate from mice, it is uncertain whether they are true across species or confined to mouse alone. Therefore, we deemed it important to study these phenomena in another species, the rat, testing the set hypothesis that AHR deficiency would afford protection against diet-induced obesity in that species as in the mouse. As the bulk of the relevant AHRKO mouse studies were conducted in male animals, we also focussed on that sex. To further facilitate comparisons with previous data, the HFD we used provided 45% of energy from fat, similarly to the case in some major mouse studies with inhibited AHR activity [15,18]. However, in contrast to the AHRKO mouse background strain (inbred C57BL/6J) that is highly obesity-prone on HFD [26], the response to HFD of the background strain for the rat AHRKO model, outbred Sprague-Dawley, is more unpredictable. Although some researchers have found Sprague-Dawley rats to be relatively well-suited to diet-induced obesity studies (with their body weight gain, however, only about half of that in Wistar rats [27]), others have reported that a substantial proportion of WT outbred Sprague-Dawley rats are resistant to dietary obesity [28] due to a polygenic pattern of resistance inheritance [29]. As a precautionary measure, we therefore provided our HFD-fed rats concomitantly free access to a 10% sucrose solution. HFD combined with high fructose/glucose in drinking water has been shown optimal for producing non-alcoholic steatohepatitis in mice [30]. Furthermore, consumption of sucrose-sweetened water, but not equivalent levels of solid sucrose, led to body fat gain in C57BL/6 mice [31].

2. Materials and methods

2.1. Experimental animals

A pair of homozygous Sprague-Dawley AHRKO rats was purchased from SAGE/Horizon Labs (Horizon Discovery, Saint Louis, MO, USA). Due to the information obtained from the provider that these rats might carry *Entamoeba muris* protozoa, heterozygous founder animals for a breeding colony were produced by mating the male AHRKO rat with WT female Sprague-Dawley rats and transferring the embryos into the uteri of recipient rats. The experimental animals were offspring of these heterozygotic parents with an *Ahr* mutant allele. Genotyping of pups was carried out by conventional PCR on DNA samples acquired through auricular piercing at pup marking. Sanger sequencing revealed that the in-house-bred homozygous AHRKO progeny were totally devoid of exon 2 in their *Ahr* gene. The WT controls in the study were littermates of the AHRKO rats. At the beginning of the study, all the 32 male rats included were 7–8 weeks old. The rats were humanely treated so that pain, suffering and distress were minimized throughout the study including the euthanization phase. The experiment was approved by the Laboratory Animal Center of the University of Helsinki. No external approval was necessary since the experiment was of non-invasive nature.

2.2. Study design

The animals were assigned into four experimental groups: WT-SD (5 rats), WT–HFD (10 rats), AHRKO–SD (7 rats), and AHRKO–HFD (10 rats). All 32 rats were housed singly in individually ventilated plastic cages (Sealsafe IVC Blue Line or Green Line IVC Sealsafe PLUS Rat, Techniplast, West Chester, PA, USA), initially with two drinking bottles (see below), and maintained on a 12-h light/dark cycle (lights on 06:00−18:00). The cage floor was covered with aspen wood bedding (Tapvei, Estonia), and each cage was enriched with a transparent red plastic hiding tube, nesting material and chew blocks (both aspen wood, Tapvei, Estonia). When the rats reached the weight of 600 g, they were transferred into a larger cage of the same brand with only one drinking bottle. The animal room temperature was kept at 22±1°C and the relative humidity at 38–75% (typically 50%).

The rats had free access to feed and drink for the entire duration of the study (24 weeks). The diets provided were manufactured by Research Diets Inc. (New Brunswick, NJ, USA). The HFD (D12451) contained 4.7 kcal/g, with 45% of the energy from fat, 20% from protein and 35% from carbohydrate. Its vitamin A concentration was 4,660 IU/kg. The SD (D12450B) contained 3.82 kcal/g, of which 10% from fat, 20% from protein and 70% from carbohydrate; it provided 3790 IU vitamin A/kg diet. For drink, the animals fed on HFD were supplied with one bottle of 10% sucrose solution and one bottle of tap water until the rats reached the weight of 600 g, after which they were offered the sucrose solution alone because the cage type only allowed suspension of a single bottle. The SD fed rats were initially supplied with two bottles of tap water and later on, if their weight exceeded 600 g, with a single water bottle.

The body weight of each animal was measured weekly. Intake of food and drink (over 24 h) was measured four times during the study (at 2, 10, 11 and 21 weeks). At week 24, the rats were fasted for about 6 h and euthanized with CO_2 followed by exanguination through the right cardiac ventricle and tissue harvesting. The order of euthanization of the animals was determined by alternation among the four groups and randomization within the groups. Samplings were conducted during three consecutive days.

2.3. Tissue samples

In addition to the carcass, the following tissues were weighed: liver, interscapular brown adipose tissue (BAT), epididymal white adipose tissue (WAT), inguinal WAT and brain. Serum was separated, and together with samples of liver, BAT and skeletal muscle (from the back of thigh), flash-frozen in liquid nitrogen and then stored at -70°C until analyses. Furthermore, pieces of liver and epididymal WAT were also fixed in 10% buffered formalin before being processed for histopathological evaluation.

2.4. Analytical methods

2.4.1. Serum clinical chemistry

Clinical chemistry analyses on serum were carried out at the Central Laboratory of the Department of Equine and Small Animal Medicine, University of Helsinki. Enzymatic methods were used for the determination of serum free fatty acids (NEFA-C, Waco Chemicals GmbH, Neuss, Germany), glycerol and D-3-hydroxybutyrate (Glycerol [GPO-PAP] and RANBUT [3-HB], Randox Laboratories Ltd. Crumlin, UK). These analyses were performed with an automatic chemistry analyser (Konelab 30*i*, Thermo Fisher Scientific). The rest of the serum analytes [alanine aminotransferase (ALT), aspartate aminotransferase (AST), bile acids, creatinine, glucose, triglycerides,

cholesterol and urea] were analysed using the reagents and adaptations recommended by the manufacturer of the automatic chemistry analyser (Konelab 60*i*, Thermo Fisher Scientific).

2.4.2. mRNA expression levels

Total RNA was reverse transcribed to cDNA at 50°C for 1 h using M-MLV RT RNase H-Point Mutant (Promega, Fitchburg WI, USA). Quantitative real-time PCR (qPCR) was performed using HOT FIREPol EvaGreen qPCR Mix Plus (no ROX; Solis Biodyne, Tartu, Estonia) on Rotor-Gene 3,000 or Rotor-Gene Q instruments (Qiagen, Hilden, Germany). This was carried out by absolute quantification, using the diluted total cDNA amount for normalization (20 ng/reaction, quantity assumed based on the original amount of RNA in RT reactions) [32,33]. Each cDNA sample was run in a duplicate reaction to obtain technical replicates. No-template controls were included in each run to control for reagent contamination. Primer specificity was confirmed by melt curve analysis at the end of each run. If the RT-qPCR result was below the detection limit, a conservative approach was taken and the sample was given the value of the limit.

Primer sequences, amplicon lengths and amplification efficiencies are shown in Supplementary Table S1. Standard curves were constructed for each primer pair by preparing a 10-fold dilution series starting from known concentrations of isolated and purified target gene PCR products amplified from cDNA samples, using the same primers as for RT-qPCR.

2.4.3. Retinoid analysis

Concentrations of ATRA, 13-cis-retinoic acid (RA13C), 9-cis-4-oxo-13,14-dihydro retinoic acid (CORA), REOH and REPA were measured in liver samples as previously described [34]. These analyses were carried out on liver samples from all rats of the SD-fed groups and 6 randomly selected rats from each of the HFD-fed groups. The different retinoid forms, extracted from liver homogenates, were separated on HPLC and detected by UV at 340 nm for the polar retinoic acid derivatives (ATRA, RA13C and CORA) [35], and at 325 nm for the apolar retinoid forms REOH and REPA [36]. Briefly, 300 mg of liver was homogenised with 300 μl of water, and retinoids were extracted with isopropanol from 400 μl of the homogenate. Separation of polar from apolar retinoid forms was achieved by solid-phase-extraction using an aminopropyl-phase cartridge (Agilent SampliQ amino, Agilent, Santa Clara, CA, USA) [35].

Analytes were separated on a Poroshell 120 EC-C18 column (Agilent) using a binary HPLC system (Agilent 1100 series, Agilent). Retinoid standards included RA13C, ATRA, REPA and REOH from Sigma-Aldrich (Madrid, Spain), whereas acitretin and retinyl acetate (Sigma-Aldrich) were used as internal standards. The retinoic acid metabolite CORA was not commercially available (see [35] for quantification details).

The limit of detection (LOD) was 0.6 pmol/g for ATRA, 0.5 pmol/g for RA13C, 1 pmol/g for CORA, and 5.6 pmol/g for REOH and REPA [35].

2.4.4. Histopathological analysis

The formalin-fixed samples of liver and epididymal WAT were embedded in paraffin, sectioned at 4 μm thickness and stained with haematoxylin-eosin for histopathological evaluation at the Finnish Centre for Laboratory Animal Pathology (FCLAP), HiLIFE, University of Helsinki. The sections were read blinded to the diet and AHR status of the animals. In the liver, steatosis (0-3; no, minimal, mild, moderate) and inflammation (0–3) were semi-quantitatively graded. In epididymal WAT, inflammatory activity and adipocyte size were estimated: The total number of crown-like structures [37] in each section (approximately equal-sized sections) was counted and the mean and median surface area and the circular diameter of adipocytes [38] per each section calculated. The adipocyte assessment was based on three representative photomicrographs (878×658 μm) captured with a 10x objective, in which the fat cells were automatically identified and their area initially measured using the Adiposoft [39] plugin of the Fiji ImageJ image processing program [40], version 1.53c. After automated analysis with Adiposoft, the resultant tagged photomicrographs and measurement tables were inspected, and erroneous adipocyte hits removed manually. After manual curation, the three analysed photomicrographs contained 130–286 quantifiable adipocytes in total [38] depending on the adipocyte size and section quality. One animal (347; Supplementary Table 3) with dense mononuclear infiltrates in the adipose tissue was left out of the adipocyte area analysis due to widespread breakage of cell membranes.

2.4.5. Statistics

The data are provided as mean±SEM. The majority of the parameters measured were subjected to two-way analysis of variance (ANOVA) with diet and genotype as independent variables. The normality of data distribution was analysed by Shapiro-Wilk's test for each cell of the design, outliers were detected by boxplots, and variance homogeneity was evaluated by Levene's test. In the case of skewed data distribution, extreme outliers, or non-homogeneous variances, log10 and square root transformations were attempted. If these failed to rectify the issue, the outliers were converted to less extreme values retaining their original ranks, and/or the data were assessed both with and without these outliers. In cases where the interaction term proved significant, simple main effects were next analysed using the pooled error term, otherwise main effects were evaluated using unweighted marginal means. In a single case (*Tnfa* expression), variance non-homogeneity was recalcitrant to all rectification attempts. Therefore, a significant two-way interaction was there followed by Welch's robust one-way ANOVA and Games-Howell's multiple comparisons.

Body weight development and the contributions of diet and sucrose for total energy intake of HFD-fed rats were statistically assessed by mixed three-way ANOVAs. Data distribution, outliers and homogeneity of variances were analysed and treated as above. The assumption of sphericity was tested by Mauchly's test of sphericity and Greenhouse-Geisser correction was used when appropriate. Major histopathological findings were graded and statistically evaluated using the Kruskal-Wallis non-parametric ANOVA on ranks except for adipocyte size measurements which were analysed by two-way ANOVAs. Finally, possible differences among the groups in vitamin A intake were tested (in addition to two-way ANOVA) by one-way ANOVA followed by the Student-Newman-Keuls post-hoc test, after verifying the assumptions as described for two-way ANOVA. These statistical analyses were conducted with the SPSS software (IBM SPSS Statistics for Windows, Version 24.0 or 25.0, Armonk, NY, USA), and the level of statistical significance was always set at $P \leq .05$.

3. Results

3.1. Feeding and drinking

Throughout the 24-week study and independent of genotype, rats on HFD consumed more energy than their counterparts on SD, as evidenced by 24-h energy intakes measured on four occasions in the course of the study (Fig. 1). While the rats on SD ate on average 70–80 kcal/day, HFD feeding raised this value to 100–110 kcal/day at 2 weeks, and to 130–150 kcal/day thereafter. This subsequent elevation was not attributable to increased eating but to increased drinking. Whereas the rats fed with SD had only water to drink, those fed with HFD could freely select between water and 10% sucrose solution, up to the point that they reached the weight of 600 g (from there on, the sucrose solution was their only option). Both WT and AHRKO rats kept their HFD intake stable over the course of the study but substantially elevated their sucrose drinking. This manifested itself as a steady rise in the contribution of sucrose to the total energy intake, reaching an equal level to the diet by 21 weeks (Supplementary Fig. S1). This change was evident as a highly significant ($P<.001$) energy source x time interaction term by mixed ANOVA. It occurred at the expense of water uptake: while the HFD-fed rats drank some 50% of the volume consumed by SD-fed rats at 2 weeks, by 10 weeks their water consumption had diminished to about 25% of their SD-fed partners (Supplementary Fig. S2). Water consumption could not be determined at the last time point (21 weeks) for HFD-fed rats because the majority of them were then provided only sucrose for drink.

3.2. Body weight development and relative organ weights

In the light of their elevated energy consumption, it was surprising that the rats fed with HFD did not gain any more weight than SD-fed rats during the study period (Fig. 2). Although a subtle tendency towards higher body weights in HFD vs. SD rats was seen by the end of the study, both a three-way mixed ANOVA over all body weight data and a two-way ANOVA on body weight change (100*[terminal BW – initial BW]/initial BW) showed that the differences among the groups failed to reach statistical significance.

A genotype-based difference was recorded in relative liver weight, which was lower in AHRKO vs. WT rats (Fig. 3). In contrast, relative interscapular BAT and epididymal WAT weights exhibited diet dependency, being heavier in rats on HFD vs. SD. No difference was detected in relative weights of inguinal (subcutaneous) WAT and brain (brain data not shown).

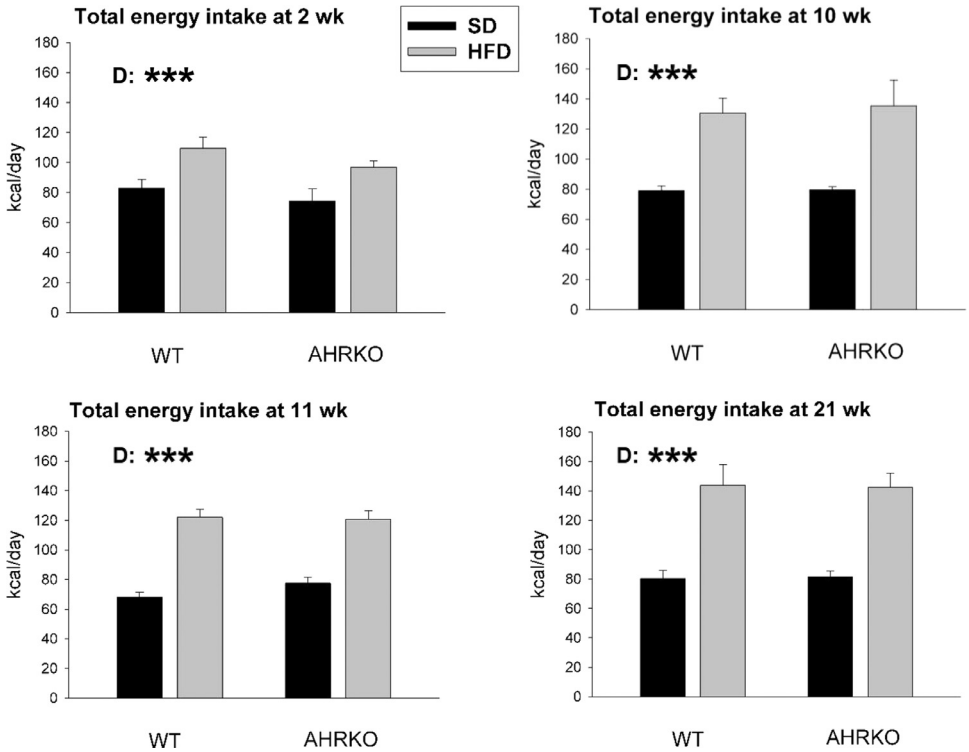

Fig. 1. Daily energy consumption of WT and AHRKO rats fed with SD or HFD (mean+SEM). In all cases, the interaction term was non-significant as assessed by ANOVA, but the main effect of diet (D) was highly significant (***: $P \leq .001$). The number of rats was 5, 7, 10 and 10 for WT-SD, AHRKO-SD, WT-HFD and AHRKO-HFD, respectively.

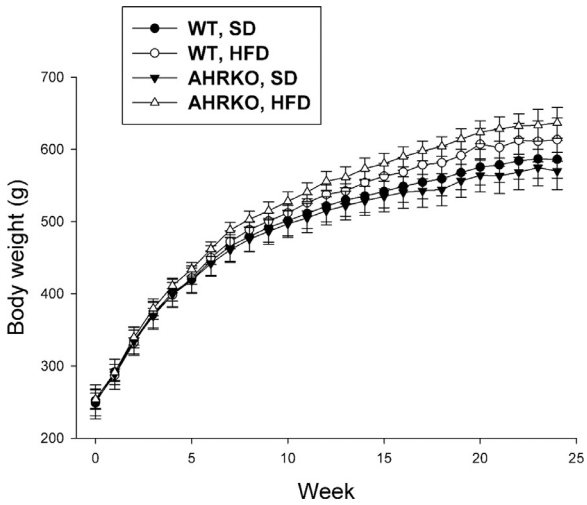

Fig. 2. Body weight development in the experimental groups during the study period (mean±SEM). Note that the Y axis scale does not contain zero. The number of rats was 5, 7, 10 and 10 for WT-SD, AHRKO-SD, WT-HFD and AHRKO-HFD, respectively.

3.3. Clinical chemistry

Of the serum biochemical variables analysed, only urea displayed a significant genotype x diet interaction. This turned out to be attributable to HFD-fed AHRKO rats, which exhibited an elevated urea concentration compared with both their genotype and dietary controls (Fig. 4). Another index of renal function, creatinine concentration, was higher in rats on HFD vs. SD. This was also true of two indices of energy metabolism, the ketone body 3-OH-butyrate and glucose. Glucose values were further slightly higher in AHRKO than WT rats. The converse was true of serum glycerol concentrations. No differences existed in free fatty acids, triglycerides, cholesterol, ALT, AST, or bile acids (data not shown).

3.4. Histopathology

In the liver, most of the rats exhibited variable glycogen accumulation and very lenient (mainly macrovesicular) steatosis (Supplementary Table S2). Other findings included occasional focal hepatocyte foaming or vacuolation and modest infiltration of inflammatory cells. One rat (in the WT-SD group) exhibited moderate focal inflammation and one rat (in the AHRKO-HFD group) had a focally extensive subcapsular necrosis. No statistically significant differences existed among the groups.

In epididymal WAT, the number of crown-like structures (as an index of adipose inflammation severity [37]) showed no connection with the genotype or diet of the rats (Supplementary Table S2). In contrast, there was a statistically significant main effect of diet ($P<.05$) on adipocyte size, whether assessed by area or circular diameter, with the HFD-fed rats exhibiting larger cells (Supplementary Fig. S3). Furthermore, this outcome was independent of the use of the mean or median of the analysed adipocytes (median not shown).

3.5. Liver retinoids and vitamin A intake

Of the five hepatic retinoids measured, none displayed a statistically significant interaction between diet and genotype. However, for REPA and CORA diet dependency was evident, with rats on HFD harbouring lower concentrations of them compared with SD-fed rats (Fig. 5). A similar tendency was observed for REOH ($P=.056$).

The same patterns emerged in total retinoid quantities in the liver: no statistically significant interactions existed, but for both

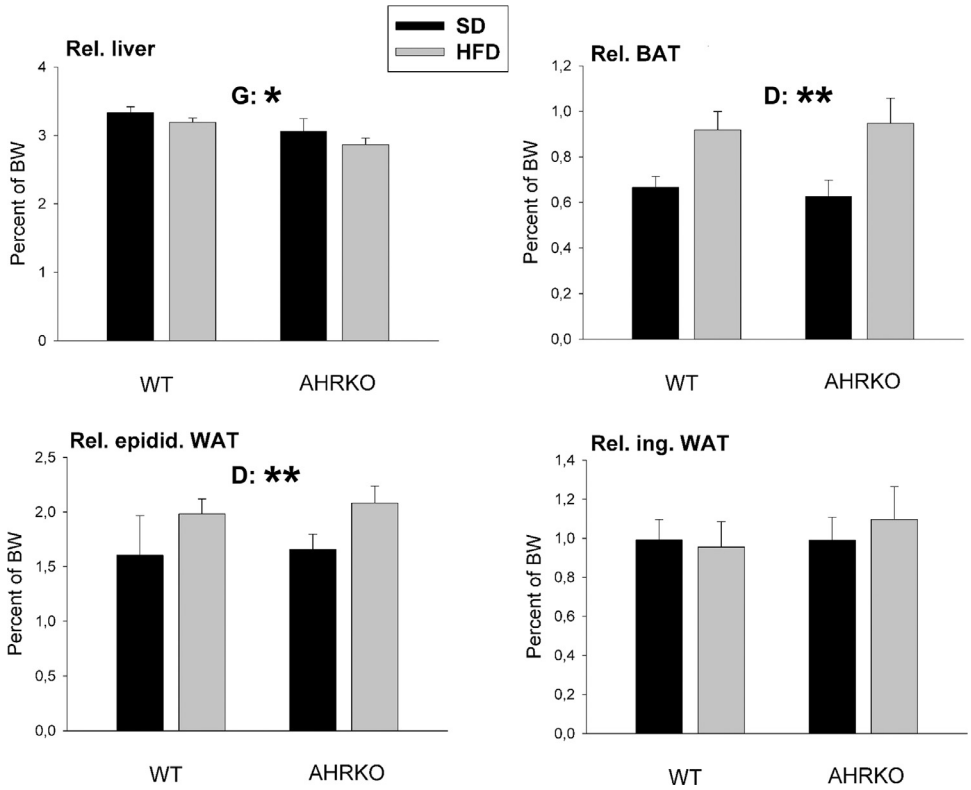

Fig. 3. Liver, interscapular BAT and epididymal & inguinal WAT weights relative to terminal body weight (mean+SEM). In all cases, the two-way interaction was non-significant as assessed by ANOVA, but the main effects of genotype (G) or diet (D) proved significant for some of the tissues (*: $P \leq .05$; **: $P \leq .01$). The number of rats was 5, 7, 10 and 10 for WT-SD, AHRKO-SD, WT-HFD and AHRKO-HFD, respectively (for liver in AHRKO-HFD, n=9).

REPA and CORA, diet displayed a significant main effect (Supplementary Fig. S4). Again, the levels were higher in rats fed with SD compared with those on HFD.

Mean intake of vitamin A (±SEM; IU) in the experimental groups over the four 24-h consumption measurements was 308±10.9, 275±10.7, 311±12.3, and 312±19.0 for WT-SD, WT-HFD, AHRKO-SD and AHRKO-HFD, respectively. These values did not differ significantly as assessed by either two- or one-way ANOVAs.

3.6. Transcripts related to energy metabolism

3.6.1. BAT transcripts

In BAT, a statistically significant interaction between diet and genotype occurred for *Ucp1, Acox1* and *Ppard*. In all of these cases, a different experimental group stood out from its diet and genotype controls: AHRKO-HFD, WT-SD or AHRKO-SD, respectively (Fig. 6). For *Pgc1a* and *Cd36*, a genotype-related difference existed in BAT, with AHRKO rats having a higher transcript abundance than WT rats. For *Ppara*, AHRKO rats similarly exhibited greater gene expression vs. WT rats (non-significant), but concomitantly HFD feeding displayed a repressing influence on this gene.

3.6.2. Liver transcripts

A significant two-way interaction was found for *Ucp2, Cpt1a2* and *Cd36*. In all of these cases, simple main effect analysis revealed that the AHRKO-HFD group had a higher gene expression level than its counterpart – either AHRKO-SD (*Ucp2* & *Cd36*) or WT-HFD (*Cpt1a2*).

Expression of the *de novo* fatty acid biosynthesis genes *Scd1* and *Elovl6* was repressed by HFD feeding, whereas it promoted *Pparg* expression. The AHRKO genotype was associated with diminished *Ppard, Acox1* and (to a lesser degree) *Elovl6* expression.

No statistically significant difference in abundance among the groups was found for the following hepatic mRNAs: *Hmgcs2, Acaca, Pgc1a, Per1, Pdk4, Fasn, Sirt1, Sirt3, Fgf21, Rictor*, and *Ppara*; the levels of *Cyp1b1* were below the detection limit. For the sensitive indicator of AHR activity, *Cyp1a1*, the mRNA concentration was below the detection limit in 18/20 AHRKO rats (being very close to it in the remaining 2 individuals), whereas it was above the detection limit in all but one WT rats (data not shown).

3.6.3. Muscle transcripts

The abundances of four skeletal muscle mRNAs were assessed (*Ucp2, Pgc1a, Ppara* and *Ppard*). Of these, the only significant finding was a slight main effect of diet on *Ucp2* expression (P=.040), with rats on HFD showing higher levels than those on SD (Supplementary Fig. S5) (Fig. 7).

3.7. Liver transcripts related to inflammation

Both the pro-inflammatory gene *Il1b* and the anti-inflammatory *Il10* showed conspicuously similar expression patterns, with the AHRKO-HFD group having 1.5–2.5 times as high mRNA levels as all the other experimental groups (Fig. 8). Also, *Tnfa* resembled them, but here the AHRKO-HFD group only differed from its diet control. Neither genotype nor diet influenced the expression of *Pgts2* or *Socs3*.

4. Discussion

Overweight, obesity and the comorbidities associated with them (the metabolic syndrome) constitute one of the most concerning public health problems globally today, and have there-

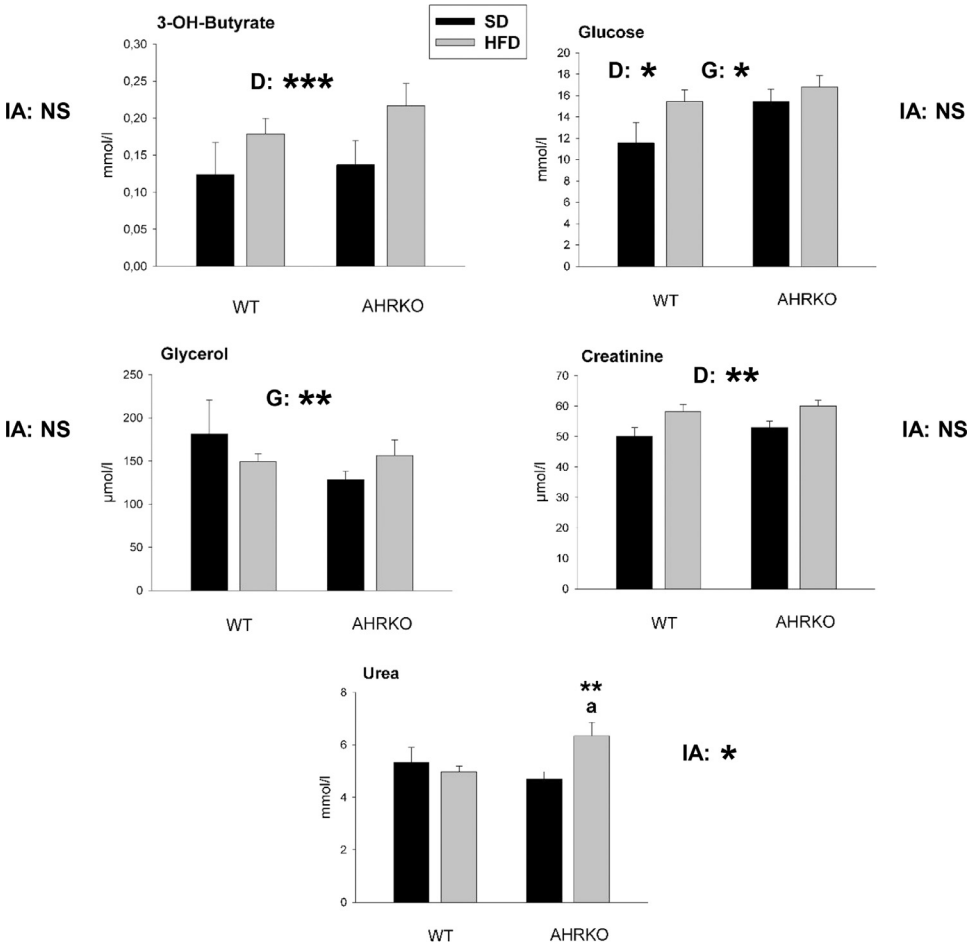

Fig. 4. Serum concentrations of 3-OH-butyrate, glucose, glycerol, creatinine and urea (mean+SEM). The data were statistically assessed by two-way ANOVA. IA: interaction; NS: non-significant; D: diet main effect; G: genotype main effect. Asterisks denote statistical significance (*: $P \leq .05$; **: $P \leq .01$; ***: $P \leq .001$). In the urea panel, the asterisks indicate a difference in simple main effects vs. diet control (AHRKO rats on SD) and the lowercase letter "a" vs. genotype control (WT rats on HFD; $P \leq .05$). The number of rats was 5, 7, 10 and 10 for WT-SD, AHRKO-SD, WT-HFD and AHRKO-HFD, respectively.

fore sparked exploration for novel treatments. A number of studies have consistently shown that AHR activity is required for diet-induced obesity to evolve, and by inhibiting AHR activity, superfluous body weight gain can be prevented [14–18]. Whether these exciting findings on AHR are specific to mouse alone or applicable across species is currently unknown. However, there are epidemiologic data associating serum AHR agonist levels with manifestations of the metabolic syndrome in humans [41,42]. Very recently, upregulation of *AHR* expression was also reported in blood cells of obese children [43]. Therefore, we set out to examine the effects of HFD in AHRKO rats.

The background strain of the rat AHRKO model, Sprague-Dawley, often shows resistance to diet-induced obesity [28], and we therefore combined HFD-feeding with provision of liquid sucrose. The higher consumption of dietary energy in the HFD vs. SD groups throughout the study failed to induce obesity in HFD-WT rats. Since calories originating from fat are more efficient for the animal than calories from carbohydrate [44], the difference in utilizable energy was initially even larger between the dietary groups, but moderated with the increasing uptake of liquid sucrose by HFD-fed rats in the course of the study. Because there was no genotype-related difference in either energy intake or body weight gain, it can be concluded that at least AHR deficiency did not interfere with the mechanism(s) of the natural resistance of Sprague-Dawley rats.

Despite similar body weight development, the experimental groups still exhibited both diet- and genotype-dependent effects in organ weights and biochemical analytes, some of which suggested marked differences between mouse and rat AHRKO models. The HFD-fed rats proved to harbour a larger epididymal WAT mass along with larger adipocytes compared with SD-fed rats. The fact that this mass difference did not extend to subcutaneous inguinal WAT is not unprecedented because their growth is fundamentally different (predominantly by hypertrophy for the epididymal fat depot but by hyperplasia for inguinal WAT [45]), and they have different metabolic roles [46]. For example, diabetes induces a drastically more severe reduction in subcutaneous compared with epididymal fat in rats [47].

In line with epididymal WAT, also interscapular BAT weight was affected by the HFD. Enlarged BAT mass in the context of obesity primarily reflects lipid content [44], but because HFD-fed rats in the present study were not obese, it might represent a marker of induced thermogenic activity, keeping in mind that BAT is central to diet-induced thermogenesis in rodents [48]. This is particularly true of AHRKO-HFD rats in which the expression of the critical oxidative phosphorylation-uncoupling gene, *Ucp1*, was also increased. A contributing factor may have been sucrose drinking which promotes BAT development in rats [49]. AHRKO rats on both diets showed high expression levels for the major mitochondrial biogenesis regulator gene, *Pgc1a*, the fatty acid transporter *Cd36*, and the

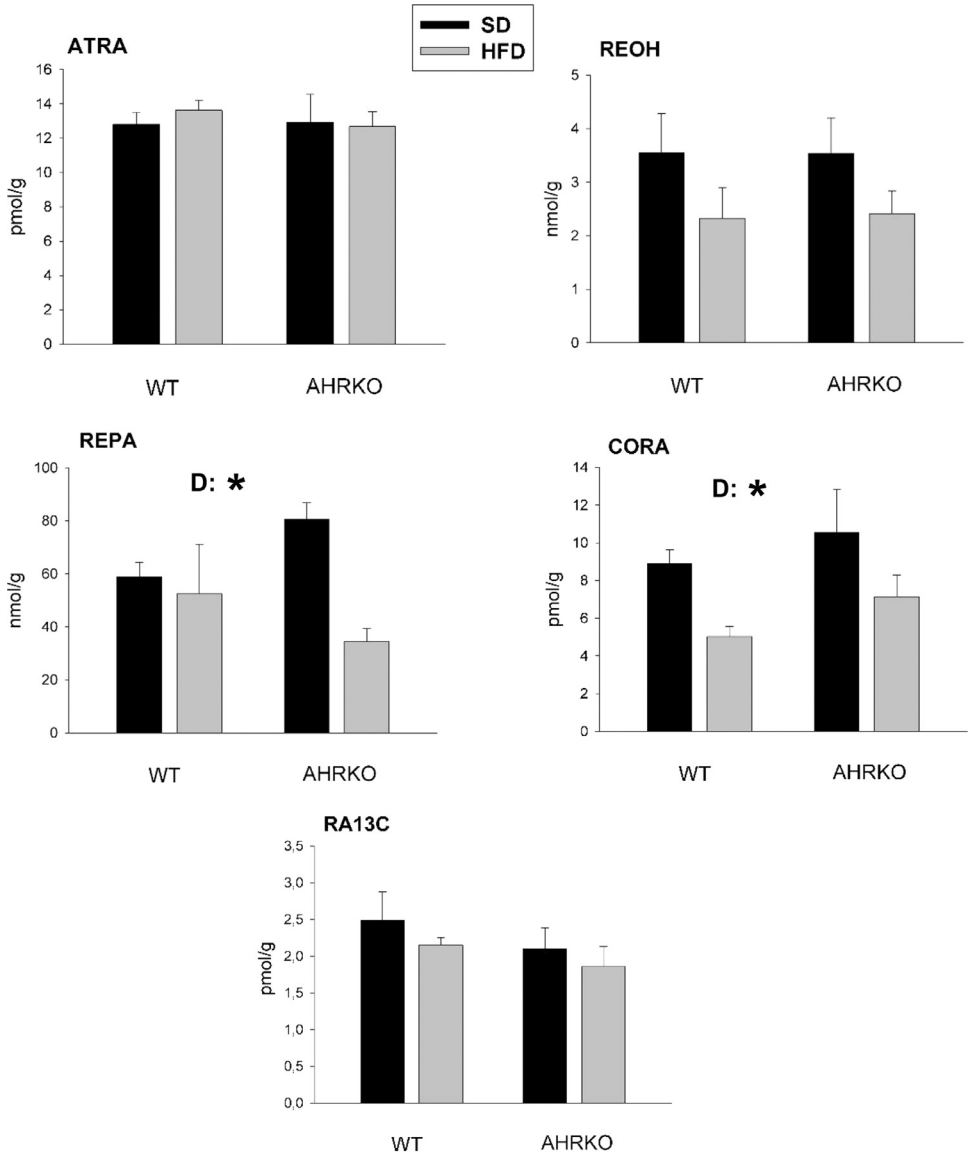

Fig. 5. Hepatic retinoid concentrations (mean+SEM). In all cases, the two-way interaction was non-significant as assessed by ANOVA, but the main effect of diet (D) proved significant for REPA and CORA (*: $P \leq .05$; **: $P \leq .01$). The number of rats was 5, 7, 6 and 6 for WT-SD, AHRKO-SD, WT-HFD and AHRKO-HFD, respectively.

important regulator of fuel oxidation, *Ppara*. This suggests that they are well endowed with the necessary tools to activate the thermogenetic machinery if necessary. The protection of WT Sprague-Dawley rats from overweight on HFD, in turn, could be related to their prominent expression of muscular *Ucp2*. Although the main role of *Ucp2* may not be in the regulation of energy metabolism but rather in protection from oxygen radicals, the protein product of this gene is able to uncouple ATP production from mitochondrial respiration [50,51].

In the liver, *Ucp2* expression was again elevated on HFD, but this time in AHRKO rats alone, which further exhibited a high expression level of *Cpt1a2*, encoding carnitine palmitoyltransferase I. This enzyme plays a pivotal role in the regulation of mitochondrial fatty acid oxidation [52]. On the other hand, *Acox1*, a rate-limiting enzyme in peroxisomal fatty acid β-oxidation, showed low expression levels in AHRKO rats in the liver, but high in BAT – in both cases irrespective of diet. There is a major difference between these two organelles in the substrates they use: While mitochondria oxidize long-chain fatty acids, the substrates of peroxisomes are very long-chain (>22 carbons) fatty acids, branched-chain fatty acids, and some leukotrienes and prostaglandins. Moreover, peroxisomal β-oxidation is essentially involved in biosynthesis pathways, while the mitochondrial pathway is related to catabolism and energy production [53]. Interestingly, eating the HFD raised BAT *Acox1* expression in WT rats to the same high level at which AHRKO rats expressed it on both diets. There may thus be a major genetic difference between AHRKO and WT rats as regards hepatic and BAT lipid metabolism.

In AHRKO rats, hepatic expression of the fatty acid transporter *Cd36* was also increased. In mice, AHR *activation* has been associated with induced *Cd36* expression and fatty acid uptake [54], albeit HFD feeding per se may also boost *Cd36* expression in mice [55]. Concomitantly here, expression of genes participating in fatty acid synthesis was either repressed (*Scd1, Elovl6*) or unchanged (*Acaca, Fasn*). This is consistent with the conclusion of a previous study in rats: "Diet-induced thermogenesis, in contrast to cold-induced non-shivering thermogenesis does not lead to increased fatty-acid synthesis and this is presumably due to the inhibitory

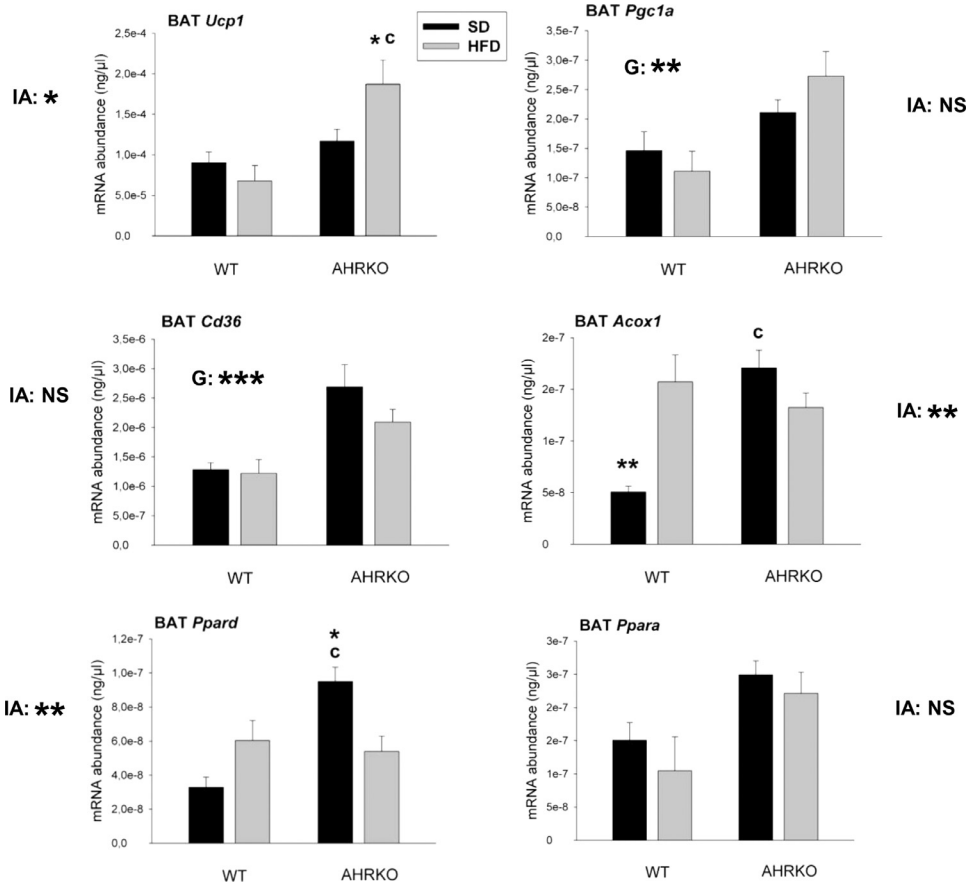

Fig. 6. Abundances of transcripts for Ucp1, Pgc1a, Cd36, Acox1, Ppard and Ppara in interscapular BAT (mean+SEM). The data were statistically assessed by two-way ANOVA. IA: interaction; NS: non-significant; G: genotype main effect. Asterisks denote statistical significance (*: $P \leq .05$; **: $P \leq .01$; ***: $P \leq .001$). For transcripts with a significant interaction term, the asterisks indicate a difference in simple main effects vs. diet control and the lowercase letters vs. the opposite genotype on the same diet (b: $P \leq .01$; c: $P \leq .001$). The number of rats was 5, 7, 10 and 10 for WT-SD, AHRKO-SD, WT-HFD and AHRKO-HFD, respectively.

effects on lipogenesis of the high dietary fat intake characteristic of cafeteria diets" [56]. Of particular interest among these genes is *Elovl6*, because the AHRKO genotype was found to potentiate the HFD-related reduction in its expression. Our previous studies with TCDD had revealed that *Elovl6* is highly inducible (˜40-fold at 4 and 10 days after exposure to 100 µg/kg) in a TCDD-sensitive rat strain but recalcitrant in a TCDD-resistant strain [57]. It thus seems to be transcriptionally regulated by AHR.

In the present study, although the histological analysis did not reveal aggravated inflammation in either the liver or WAT as opposed to findings in diet-induced obesity models [58], the HFD triggered an increased hepatic expression of the pro-inflammatory genes *Tnfa* and *Il1b* in AHRKO rats. The fact that a highly similar response also occurred in expression of the anti-inflammatory gene *Il10* may represent feedback regulation. On the other hand, induced *Il10* expression might account for the lack of discernible cellular inflammatory reaction. In any case, the transcript response suggests that, in contrast to mice, in rats AHR deficiency might render HFD-fed animals prone to immune activation in internal organs, probably through impaired intestinal barrier function [59,60]. Finding a way to cause frank obesity in WT rats (possibly by further increasing the proportion of energy acquired from fat in the HFD) would be crucial in the future for verification of this hypothesis and unobscured comparison of the mouse and rat AHRKO models.

Besides ascertaining the influence of AHRKO on HFD-induced body weight gain in rats, another objective of the present study was to find out whether the previously reported drastic changes in hepatic retinoid concentrations in an AHRKO mouse line would also occur in AHRKO rats. They could potentially bear on the beneficial metabolic impacts of AHRKO, because ATRA and its precursor, retinaldehyde, have proven to be capable of counteracting diet-induced obesity [61,62]. Although AHRKO rats exhibited unaltered hepatic retinoid levels on SD similar to a different AHRKO mouse line [24], interestingly, HFD reduced CORA and REPA concentrations with a similar tendency for REOH. In mass units, rats ate the HFD less than the SD. However, vitamin A concentration was higher in the HFD (4,660 IU/kg vs. 3,790 IU/kg), fully offsetting the consumption difference. Therefore, the diminished hepatic retinoid concentrations are unlikely to have stemmed from lowered vitamin A intake of rats on HFD. Consistent with these data, HFD feeding in two rat strains lowered REOH concentration and tended to decrease REPA concentration in the liver [63]. Likewise, both HFD-fed and genetically obese mice have been reported to harbour reduced hepatic REOH and REPA concentrations, and increasing severity of fatty liver disease in humans correlates with decreases in hepatic vitamin A [64]. Contrary to these convergent findings, however, one previous study recorded an elevated hepatic REOH concentration in HFD-fed rats. It seemed to arise as a consequence of suppressed REOH metabolism, which was partially due to increased serum cholesterol level [65]. This may account for the discrepancy inasmuch as our rats fed with HFD did not exhibit any rise in serum cholesterol.

There were, overall, relatively few statistically significant alterations in serum clinical chemistry. A notable diet-related impact

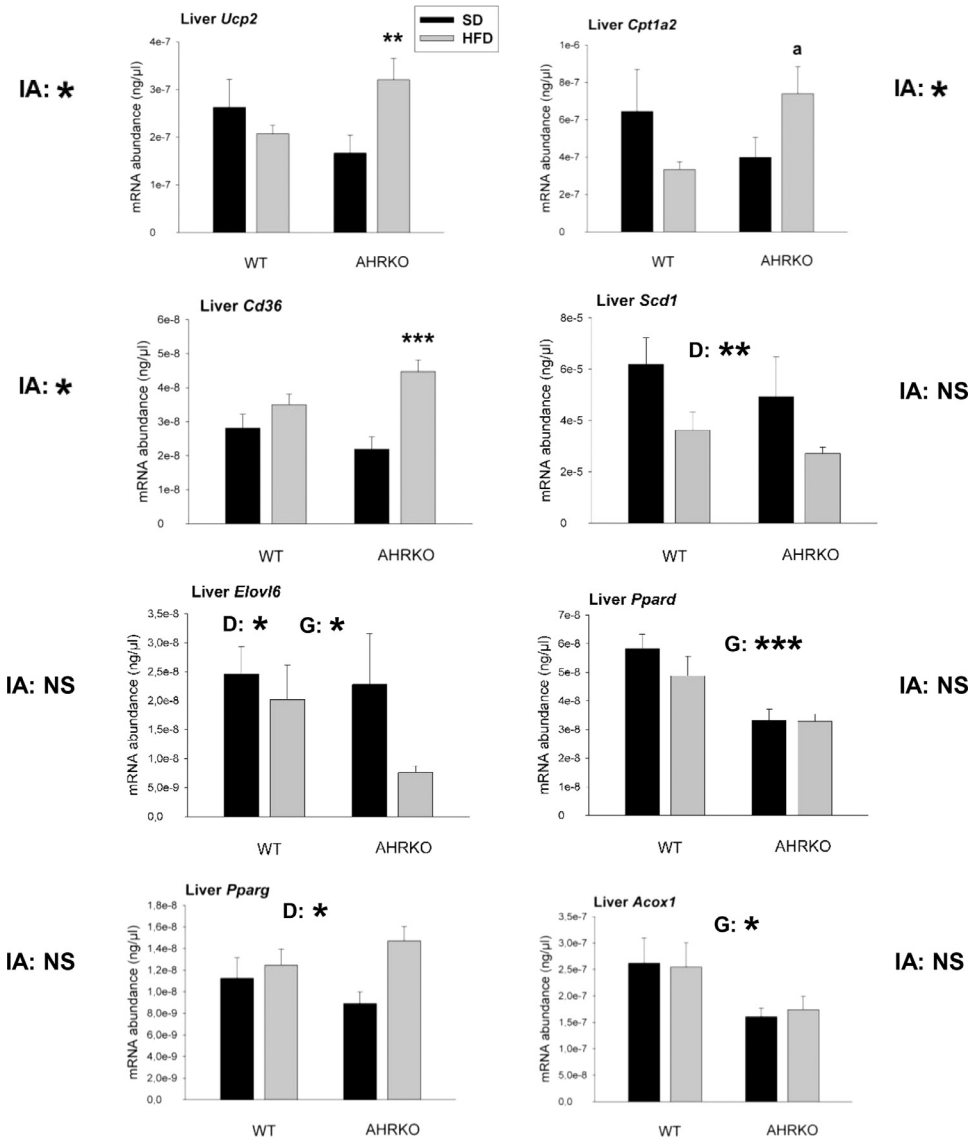

Fig. 7. Expression of genes related to energy balance in the liver (mean+SEM). The data were statistically assessed by two-way ANOVA. IA: interaction; NS: non-significant; D: diet main effect; G: genotype main effect. Asterisks denote statistical significance (*: $P \leq .05$; **: $P \leq .01$; ***: $P \leq .001$). For transcripts with a significant interaction term, the asterisks indicate a difference in simple main effects vs. diet control and the lowercase letter "a" vs. the opposite genotype on the same diet ($P \leq .05$). The number of rats was 5, 7, 10 and 10 for WT-SD, AHRKO-SD, WT-HFD and AHRKO-HFD, respectively.

was seen in 3-OH-butyrate, which was considerably increased in rats fed on HFD in accordance with the high fat content of their feed. Concomitantly, these rats also exhibited an increase in serum glucose probably due to their sucrose drinking. Glucose levels were slightly higher and glycerol levels lower in AHRKO than WT rats, which might suggest more active gluconeogenesis in the former. Although circulating creatinine concentration was elevated by the HFD, frank renal damage is unlikely in WT rats due to lack of dyslipidemia [66] and of a parallel change in serum urea. In contrast, AHRKO rats displayed elevated serum urea concentration, which probably reflects the established occurrence of subclinical hydronephrosis and -ureter in this animal model [67].

Previously, the protection of AHRKO mice from obesity and hepatic steatosis on HFD was found to be associated with augmented expressions of *Socs3, Fgf21, Cyp1b1, Scd1* and PPARα target genes (such as *Cd36, Cpt1a* and *Elovl6*). Wada et al. [20] showed that while HFD induced hepatic *Socs3* expression, liver-specific AHRKO attenuated it, concomitantly exacerbating HFD-triggered steatohepatitis. *Socs3* proved to be a transcriptional target of AHR, and a rescue of *Socs3* expression restored the liver status in terms of fat content and inflammation to on par with that in WT mice. Also employing liver-specific AHRKO (though inducible in this case), Girer et al. [68] reported a sexually dimorphic influence of AHRKO in mice, with body weight gain being suppressed by AHRKO on both SD and HFD in females alone. A key mediator role was proposed for *Fgf21*, whose liver expression was doubled in AHRKO mice. Mice inducibly deficient of both AHR and FGF21 gained weight faster on SD than their WT controls. Most recently, it was found that HFD induced the hepatic gene expression of *Cyp1b1, Scd1, Spp1* and some of PPARα target genes, whereas AHR inhibition by chemical agents reversed this [18]. Especially central for both HFD-induced obesity and its prevention by AHR was inferred to be *Cyp1b1*. In the present study, *Cyp1b1* abundance was below detection level, but none of the other hepatic genes listed above (excluding *Spp1* that was not determined) responded in the manner reported. Although the resistance to diet-induced obe-

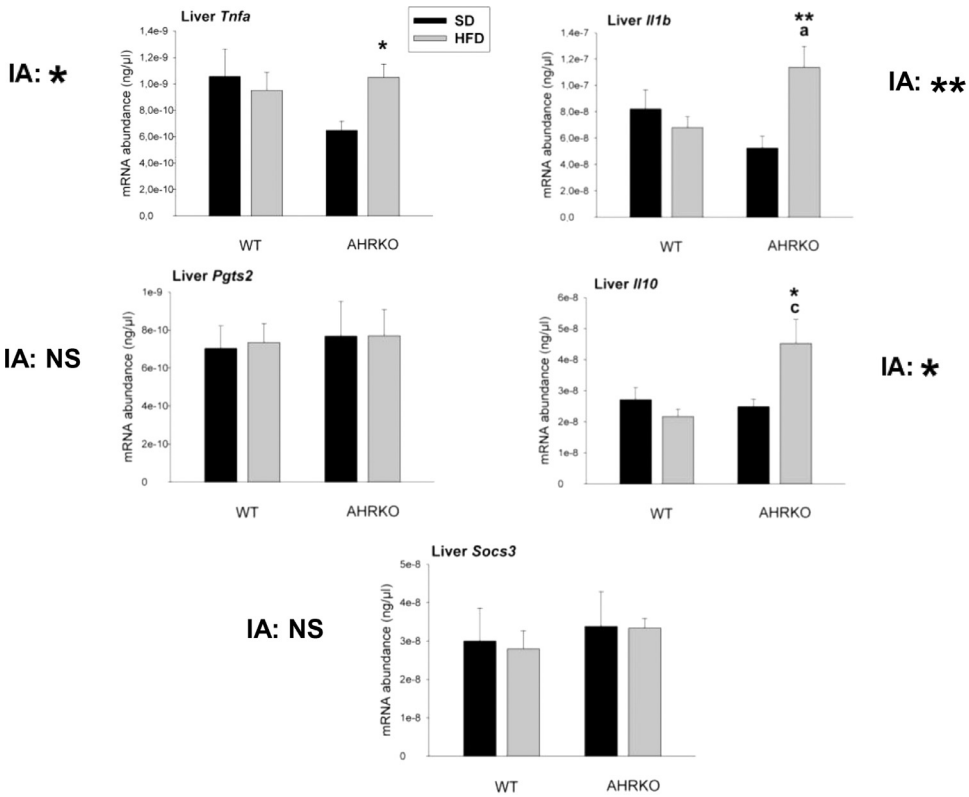

Fig. 8. Expression of genes related to inflammation in the liver (mean+SEM). The data were statistically assessed by two-way ANOVA. IA: interaction; NS: non-significant; D: diet main effect; G: genotype main effect. Asterisks denote statistical significance (*: $P \leq .05$; **: $P \leq .01$). For transcripts with a significant interaction term, the asterisks indicate a difference in simple main effects vs. diet control and the lowercase letters vs. the opposite genotype on the same diet (a, $P \leq .05$; c, $P \leq .001$). The number of rats was 5, 7, 10 and 10 for WT-SD, AHRKO-SD, WT-HFD and AHRKO-HFD, respectively.

sity shown by our rats may have contributed to the discrepant outcome, interspecies differences between mice and rats are also likely.

Finally, an interesting issue is also whether AHRKO affords any metabolic advantages in lean rats. In the present study, there were, indeed, certain *Ahr* genotype-dependent differences in metabolic variables, such as lower serum glycerol but higher glucose in AHRKO vs. WT rats. Likewise, the expression of BAT *Cd36* and *Pgc1a* was increased, while that of liver *Ppard, Elovl6* and *Acox1* was decreased in AHRKO rats compared with their WT counterparts. Further studies are needed to tease out the significance of these and other differences to the energy metabolism as a whole.

This is the first study on AHRKO rats fed with HFD. Its strengths include long exposure time, fairly high group size for HFD-fed animals and a broad spectrum of variables analysed. Limitations, in turn, include unfavourable background strain of the animal model, single sex, infrequent measurement of food and drink intakes, and lack of data on some metabolic hormones (insulin, leptin) and on glucose tolerance.

Taken together, the present study demonstrates that promoting dietary obesity in male Sprague-Dawley rats of the AHRKO background line is much more challenging than described in the literature for C57BL/6 mice, and therefore the protective effect of AHR deficiency against diet-induced obesity could not be assessed in AHRKO rats. Although body weight gain did not differ among the experimental groups, they still exhibited both diet- and genotype-dependent biochemical effects, some of which suggested marked differences between mouse and rat AHRKO models. For example, the reported alterations in gene expression of some genes suggested critical in HFD-fed AHRKO mice (such as *Socs3* and *Fgf21*) did not occur in AHRKO rats, while increased expression of inflammatory genes was recorded in AHRKO rats, but reportedly does not occur in AHRKO mice. No evidence of AHR influence on hepatic retinoid concentrations in rats was obtained, in contrast to what has been reported in a single mouse AHRKO line. Further studies are needed to elucidate the factor(s) responsible for this discrepancy.

Acknowledgments

Technical assistance by Ms. Anu Seppänen and the staff of the Laboratory Animal Centre (LAC) of the University of Helsinki is gratefully acknowledged.

Declaration of Competing Interest

The authors declare no competing interests.

Funding

This study was supported by grants from the Academy of Finland (no. 261232) and from the Foundation of the Finnish Veterinary Medicine to RP.

Supplementary materials

Supplementary material associated with this article can be found, in the online version, at doi:10.1016/j.jnutbio.2021.108762.

CRediT authorship contribution statement

Raimo Pohjanvirta: Conceptualization, Formal analysis, Writing – original draft, Supervision, Project administration, Funding acquisition. **Ira Karppinen:** Investigation. **Suylen Galbán-Velázquez:** Investigation. **Javier Esteban:** Investigation, Supervision, Writing – review & editing. **Helen Håkansson:** Supervision, Writing – review & editing. **Satu Sankari:** Investigation. **Jere Lindén:** Investigation, Writing – review & editing.

References

[1] Poland A, Glover E, Kende AS. Stereospecific, high affinity binding of 2,3,7,8-tetrachlorodibenzo-p-dioxin by hepatic cytosol. Evidence that the binding species is receptor for induction of aryl hydrocarbon hydroxylase. J Biol Chem 1976;251:4936–46.

[2] Dietrich C. The AHR in the control of cell cycle and apoptosis. In: Pohjanvirta R, editor. The AH Receptor in Biology and Toxicology. Hoboken, NJ, USA: John Wiley & Sons, Inc.; 2012. p. 467–84.

[3] Fernandez-Salguero PM. A remarkable new target gene for the dioxin receptor: The Vav3 proto-oncogene links AhR to adhesion and migration. Cell Adh Migr 2010;4:172–5.

[4] Schmidt JV, Su GH, Reddy JK, Simon MC, Bradfield CA. Characterization of a murine Ahr null allele: involvement of the Ah receptor in hepatic growth and development. Proc Natl Acad Sci USA 1996;93:6731–6.

[5] Ichihara S. Role of AHR in the development of the liver and blood vessels. In: Pohjanvirta R, editor. The AH Receptor in Biology and Toxicology. Hoboken, NJ, USA: John Wiley & Sons, Inc.; 2012. p. 413–22.

[6] Karman BN, Hernández-Ochoa I, Ziv-Gal A, Flaws JA. Involvement of the AHR in development and functioning of the male and female reproductive systems. In: Pohjanvirta R, editor. The AH Receptor in Biology and Toxicology. Hoboken, NJ, USA: John Wiley & Sons, Inc.; 2012. p. 437–66.

[7] Esser C, Rannug A. The aryl hydrocarbon receptor in barrier organ physiology, immunology, and toxicology. Pharmacol Rev 2015;67:259–79.

[8] Pohjanvirta R, Mahiout S. Aryl hydrocarbon receptor is indispensable for beta-naphthoflavone-induced novel food avoidance and may be involved in LiCl-triggered conditioned taste aversion in rats. Physiol Behav 2019;204:58–64.

[9] Moura-Alves P, Puyskens A, Stinn A, Klemm M, Guhlich-Bornhof U, Dorhoi A, et al. Host monitoring of quorum sensing during *Pseudomonas aeruginosa* infection. Science (New York, NY) 2019;366.

[10] Lee JS, Cella M, McDonald KG, Garlanda C, Kennedy GD, Nukaya M, et al. AHR drives the development of gut ILC22 cells and postnatal lymphoid tissues via pathways dependent on and independent of Notch. Nat Immunol 2011;13:144–51.

[11] Yin J, Yang K, Zhou C, Xu P, Xiao W, Yang H. Aryl hydrocarbon receptor activation alleviates dextran sodium sulfate-induced colitis through enhancing the differentiation of goblet cells. Biochem Biophys Res Commun 2019;514:180–6.

[12] Bessede A, Gargaro M, Pallotta MT, Matino D, Servillo G, Brunacci C, et al. Aryl hydrocarbon receptor control of a disease tolerance defence pathway. Nature 2014;511:184–90.

[13] Zhao X, Li J, Ma J, Jiao C, Qiu X, Cui X, et al. MiR-124a mediates the impairment of intestinal epithelial integrity by targeting aryl hydrocarbon receptor in crohn's disease. Inflammation 2020;43:1862–75.

[14] Kerley-Hamilton JS, Trask HW, Ridley CJ, Dufour E, Ringelberg CS, Nurinova N, et al. Obesity is mediated by differential aryl hydrocarbon receptor signaling in mice fed a Western diet. Environ Health Perspect 2012;120:1252–9.

[15] Moyer BJ, Rojas IY, Kerley-Hamilton JS, Hazlett HF, Nemani KV, Trask HW, et al. Inhibition of the aryl hydrocarbon receptor prevents Western diet-induced obesity. Model for AHR activation by kynurenine via oxidized-LDL, TLR2/4, TGFbeta, and IDO1. Toxicol Appl Pharmacol 2016;300:13–24.

[16] Xu CX, Wang C, Zhang ZM, Jaeger CD, Krager SL, Bottum KM, et al. Aryl hydrocarbon receptor deficiency protects mice from diet-induced adiposity and metabolic disorders through increased energy expenditure. Int J Obes 2005;39(2015):1300–9.

[17] Moyer BJ, Rojas IY, Kerley-Hamilton JS, Nemani KV, Trask HW, Ringelberg CS, et al. Obesity and fatty liver are prevented by inhibition of the aryl hydrocarbon receptor in both female and male mice. Nutr Res 2017;44:38–50.

[18] Rojas IY, Moyer BJ, Ringelberg CS, Tomlinson CR. Reversal of obesity and liver steatosis in mice via inhibition of aryl hydrocarbon receptor and altered gene expression of CYP1B1, PPARalpha, SCD1, and osteopontin. Int J Obes 2020;44:948–63.

[19] Baker NA, Shoemaker R, English V, Larian N, Sunkara M, Morris AJ, et al. Effects of adipocyte aryl hydrocarbon receptor deficiency on pcb-induced disruption of glucose homeostasis in lean and obese mice. Environ Health Perspect 2015;123:944–50.

[20] Wada T, Sunaga H, Miyata K, Shirasaki H, Uchiyama Y, Shimba S. Aryl hydrocarbon receptor plays protective roles against high fat diet (HFD)-induced hepatic steatosis and the subsequent lipotoxicity via direct transcriptional regulation of socs3 gene expression. J Biol Chem 2016;291:7004–16.

[21] Brulport A, Le Corre L, Chagnon MC. Chronic exposure of 2,3,7,8-tetrachlorodibenzo-p-dioxin (TCDD) induces an obesogenic effect in C57BL/6J mice fed a high fat diet. Toxicology 2017;390:43–52.

[22] Pohjanvirta R, Tuomisto J. Short-term toxicity of 2,3,7,8-tetrachlorodibenzo-p–dioxin in laboratory animals: effects, mechanisms, and animal models. Pharmacol Rev 1994;46:483–549.

[23] Andreola F, Fernandez-Salguero PM, Chiantore MV, Petkovich MP, Gonzalez FJ, De Luca LM. Aryl hydrocarbon receptor knockout mice (AHR-/-) exhibit liver retinoid accumulation and reduced retinoic acid metabolism. Cancer Res 1997;57:2835–8.

[24] Esteban JSI, Miettinen HM, Korkalainen M, Viluksela M, Pohjanvirta R, Håkansson H. 2,3,7,8-Tetrachlorodibenzo-*p*-dioxin (TCDD)-induced retinoid disruption: comparison between wildtype and aryl hydrocarbon receptor knockout mice. Reprod Toxicol 2021;101:33–49.

[25] Wilhelm C, Kharabi Masouleh S, Kazakov A. Metabolic regulation of innate lymphoid cell-mediated tissue protection-linking the nutritional state to barrier immunity. Front Immunol 2017;8:1742.

[26] Buettner R, Schölmerich J, Bollheimer LC. High-fat diets: modeling the metabolic disorders of human obesity in rodents. Obesity (Silver Spring, Md) 2007;15:798–808.

[27] Marques C, Meireles M, Norberto S, Leite J, Freitas J, Pestana D, et al. High-fat diet-induced obesity Rat model: a comparison between Wistar and Sprague–Dawley Rat. Adipocyte 2016;5:11–21.

[28] Levin BE, Triscari J, Hogan S, Sullivan AC. Resistance to diet-induced obesity: food intake, pancreatic sympathetic tone, and insulin. Am J Physiol 1987;252:R471–8.

[29] Levin BE, Dunn-Meynell AA, Balkan B, Keesey RE. Selective breeding for diet-induced obesity and resistance in Sprague-Dawley rats. Am J Physiol 1997;273:R725–30.

[30] Liu XJ, Duan NN, Liu C, Niu C, Liu XP, Wu J. Characterization of a murine nonalcoholic steatohepatitis model induced by high fat high calorie diet plus fructose and glucose in drinking water. Lab Invest 2018;98:1184–99.

[31] Togo J, Hu S, Li M, Niu C, Speakman JR. Impact of dietary sucrose on adiposity and glucose homeostasis in C57BL/6J mice depends on mode of ingestion: liquid or solid. Mol Metab 2019;27:22–32.

[32] Bustin SA. Quantification of mRNA using real-time reverse transcription PCR (RT-PCR): trends and problems. J Mol Endocrinol 2002;29:23–39.

[33] Tichopad A, Kitchen R, Riedmaier I, Becker C, Stahlberg A, Kubista M. Design and optimization of reverse-transcription quantitative PCR experiments. Clin Chem 2009;55:1816–23.

[34] Mahiout S, Linden J, Esteban J, Sanchez-Perez I, Sankari S, Pettersson L, et al. Toxicological characterisation of two novel selective aryl hydrocarbon receptor modulators in sprague-dawley rats. Toxicol Appl Pharmacol 2017;326:54–65.

[35] Schmidt CK, Brouwer A, Nau H. Chromatographic analysis of endogenous retinoids in tissues and serum. Anal Biochem 2003;315:36–48.

[36] van der Ven LT, van de Kuil T, Leonards PE, Slob W, Lilienthal H, Litens S, et al. Endocrine effects of hexabromocyclododecane (HBCD) in a one-generation reproduction study in Wistar rats. Toxicol Lett 2009;185:51–62.

[37] Poret JM, Souza-Smith F, Marcell SJ, Gaudet DA, Tzeng TH, Braymer HD, et al. High fat diet consumption differentially affects adipose tissue inflammation and adipocyte size in obesity-prone and obesity-resistant rats. Int J Obes 2005;42:535–41 2018.

[38] Parlee SD, Lentz SI, Mori H, MacDougald OA. Quantifying size and number of adipocytes in adipose tissue. Methods Enzymol 2014;537:93–122.

[39] Galarraga M, Campión J, Muñoz-Barrutia A, Boqué N, Moreno H, Martínez JA, et al. Adiposoft: automated software for the analysis of white adipose tissue cellularity in histological sections. J Lipid Res 2012;53:2791–6.

[40] Schindelin J, Arganda-Carreras I, Frise E, Kaynig V, Longair M, Pietzsch T, et al. Fiji: an open-source platform for biological-image analysis. Nat Methods 2012;9:676–82.

[41] Park WH, Jun DW, Kim JT, Jeong JH, Park H, Chang YS, et al. Novel cell-based assay reveals associations of circulating serum AhR-ligands with metabolic syndrome and mitochondrial dysfunction. BioFactors (Oxford, England) 2013;39:494–504.

[42] Roh E, Kwak SH, Jung HS, Cho YM, Pak YK, Park KS, et al. Serum aryl hydrocarbon receptor ligand activity is associated with insulin resistance and resulting type 2 diabetes. Acta Diabetologica 2015;52:489–95.

[43] Shahin NN, Abd-Elwahab GT, Tawfiq AA, Abdelgawad HM. Potential role of aryl hydrocarbon receptor signaling in childhood obesity. Biochem Biophys Acta Mol Cell Biol Lipids 2020;1865:158714.

[44] Trayhurn P. Origins and early development of the concept that brown adipose tissue thermogenesis is linked to energy balance and obesity. Biochimie 2017;134:62–70.

[45] DiGirolamo M, Fine JB, Tagra K, Rossmanith R. Qualitative regional differences in adipose tissue growth and cellularity in male Wistar rats fed ad libitum. Am J Physiol 1998;274:R1460–7.

[46] Tchkonia T, Thomou T, Zhu Y, Karagiannides I, Pothoulakis C, Jensen MD, et al. Mechanisms and metabolic implications of regional differences among fat depots. Cell metabolism 2013;17:644–56.

[47] Ghorbani A, Varedi M, Hadjzadeh MA, Omrani GH. Type-1 diabetes induces depot-specific alterations in adipocyte diameter and mass of adipose tissues in the rat. Exp Clin Endocrinol Diabetes 2010;118:442–8.

[48] Feldmann HM, Golozoubova V, Cannon B, Nedergaard J. UCP1 ablation induces

obesity and abolishes diet-induced thermogenesis in mice exempt from thermal stress by living at thermoneutrality. Cell Metab 2009;9:203–9.
[49] Rattigan S, Clark MG. Effect of sucrose solution drinking option on the development of obesity in rats. J Nutr 1984;114:1971–7.
[50] Schrauwen P, Hesselink M. UCP2 and UCP3 in muscle controlling body metabolism. J Exp Biol 2002;205:2275–85.
[51] Erlanson-Albertsson C. The role of uncoupling proteins in the regulation of metabolism. Acta Physiol Scand 2003;178:405–12.
[52] McGarry JD, Mannaerts GP, Foster DW. A possible role for malonyl-CoA in the regulation of hepatic fatty acid oxidation and ketogenesis. J Clin Invest 1977;60:265–70.
[53] Demarquoy J, Le Borgne F. Crosstalk between mitochondria and peroxisomes. World J Biol Chem 2015;6:301–9.
[54] Lee JH, Wada T, Febbraio M, He J, Matsubara T, Lee MJ, et al. A novel role for the dioxin receptor in fatty acid metabolism and hepatic steatosis. Gastroenterology 2010;139:653–63.
[55] Inoue M, Ohtake T, Motomura W, Takahashi N, Hosoki Y, Miyoshi S, et al. Increased expression of PPARgamma in high fat diet-induced liver steatosis in mice. Biochem Biophys Res Commun 2005;336:215–22.
[56] Rothwell NJ, Stock MJ, Trayhurn P. Reduced lipogenesis in cafeteria-fed rats exhibiting diet-induced thermogenesis. Biosci Rep 1983;3:217–24.
[57] Boutros PC, Yao CQ, Watson JD, Wu AH, Moffat ID, Prokopec SD, et al. Hepatic transcriptomic responses to TCDD in dioxin-sensitive and dioxin-resistant rats during the onset of toxicity. Toxicol Appl Pharmacol 2011;251:119–29.
[58] Muhlhausler BS, Toop C, Gentili S. Nutritional models of type 2 diabetes mellitus. Methods Mol Biol 2020;2076:43–69.
[59] Natividad JM, Agus A, Planchais J, Lamas B, Jarry AC, Martin R, et al. Impaired aryl hydrocarbon receptor ligand production by the gut microbiota is a key factor in metabolic syndrome. Cell metabolism 2018;28:737–49 e4.
[60] Postal BG, Ghezzal S, Aguanno D, André S, Garbin K, Genser L, et al. AhR activation defends gut barrier integrity against damage occurring in obesity. Mol Metab 2020;39:101007.
[61] Berry DC, Noy N. All-trans-retinoic acid represses obesity and insulin resistance by activating both peroxisome proliferation-activated receptor beta/delta and retinoic acid receptor. Mol Cell Biol 2009;29:3286–96.
[62] Ziouzenkova O, Orasanu G, Sharlach M, Akiyama TE, Berger JP, Viereck J, et al. Retinaldehyde represses adipogenesis and diet-induced obesity. Nat Med 2007;13:695–702.
[63] Shirai T, Shichi Y, Sato M, Tanioka Y, Furusho T, Ota T, et al. High dietary fat-induced obesity in Wistar rats and type 2 diabetes in nonobese Goto-Kakizaki rats differentially affect retinol binding protein 4 expression and vitamin A metabolism. Nutr Res 2016;36:262–70.
[64] Trasino SE, Tang XH, Jessurun J, Gudas LJ. Obesity leads to tissue, but not serum vitamin a deficiency. Sci Rep 2015;5:15893.
[65] Zhang M, Liu C, Hu MY, Zhang J, Xu P, Li F, et al. High-fat diet enhanced retinal dehydrogenase activity, but suppressed retinol dehydrogenase activity in liver of rats. J Pharmacol Sci 2015;127:430–8.
[66] Zhang R, Yu Y, Deng J, Zhang C, Zhang J, Cheng Y, et al. Sesamin ameliorates high-fat diet-induced dyslipidemia and kidney injury by reducing oxidative stress. Nutrients 2016;8:276.
[67] Harrill JA, Hukkanen RR, Lawson M, Martin G, Gilger B, Soldatow V, et al. Knockout of the aryl hydrocarbon receptor results in distinct hepatic and renal phenotypes in rats and mice. Toxicol Appl Pharmacol 2013;272:503–18.
[68] Girer NG, Carter D, Bhattarai N, Mustafa M, Denner L, Porter C, et al. Inducible Loss of the Aryl Hydrocarbon Receptor Activates Perigonadal White Fat Respiration and Brown Fat Thermogenesis via Fibroblast Growth Factor 21. Int J Mol Sci 2019;20:950.